Nationaal Lucht- en Ruimtevaartlaboratorium
National Aerospace Laboratory NLR

NLR-TP-2002-597

Deformation Modelling of the single crystal superalloy CM186 LC

R. Daniel, T. Tinga, M.B. Henderson and T.J. Ward

Nationaal Lucht- en Ruimtevaartlaboratorium
National Aerospace Laboratory NLR

NLR-TP-2002-597

Deformation Modelling of the single crystal superalloy CM186 LC

R. Daniel[1)] , T. Tinga, M.B. Henderson[2)] and T.J. Ward[1)]

1) QinetiQ
2) Alstom Power

This report is based on a presentation held on the COST Conference "Materials for Advanced Power Engineering 2002", at Liege on October 1, 2002.

The intention of this presentation is to give an overview of the capabilities that have been developed in the field of single crystal modelling.

Customer:	National Aerospace Laboratory NLR
Working Plan number:	S.1.B.3
Owner:	National Aerospace Laboratory NLR
Division:	Structures and Materials
Distribution:	Unlimited
Classification title:	Unclassified
	October 2002

Contents

11 Figures

(15 pages in total)

List of Symbols

ɔ	shear strain
Ůᶎ	creep strain
µ	Schmid factor matrix
ůᶷ	stress
ɓ, ə, ʂ , ɤ , S,	
S_{ss}, H, a_i, b_i, Q_i	model parameters (constants)
k	slip system index
SX	single crystal
T	temperature
t	time

DEFORMATION MODELLING OF THE SINGLE CRYSTAL SUPERALLOY CM186 LC

R. Daniel*, T. Tinga[Ψ], M.B. Henderson[+], T.J. Ward*
QinetiQ*, UK, NLR, Netherlands[Ψ], ALSTOM Power, UK[+],

Abstract

Single crystal nickel-based superalloys are being used increasingly to manufacture the turbine blades for both aero engines and land-based gas turbine engines. These alloys provide significant increases in component endurance and reliability, as well as engine performance due to the increased turbine entry temperature levels that can be achieved. To ensure full utilisation and determination of safe component lifetimes, accurate modelling of the non-linear deformation suffered during typical duty cycles is needed. In recent years a number of anisotropic creep data analysis and modelling methods have been developed, largely based on the determination of constitutive parameters for the <001> and <111> crystallographic directions. These models have been incorporated within a Schmid's Law slip-system analysis to determine local shear creep strain accumulation and resolved shear stresses. Any appropriate creep formulation can be included within this framework. The present paper describes the development of two models: i) the QinetiQ Creep Law and ii) the creep law used by the National Aerospace Laboratory NLR of the Netherlands, that have been incorporated into user material subroutines for the ABAQUS and MSC Marc finite element programmes, respectively. The models allow full three-dimensional analysis with elastic, plastic, creep and thermal deformations capable of simulating the high temperature creep and thermomechanical fatigue behaviour of specimens and turbine blades under service loading conditions. Predictions have been generated for the anisotropic creep behaviour of a number of specimen tests and blade designs for the as-cast (non-solutioned) single crystal nickel based superalloy CM186LC.

Keywords: Creep, Anisotropy, CM186LC, Single Crystal, Finite Element Analysis.

Introduction

The demands placed on gas turbine engine hot section components are extreme. Typical metal temperatures range from 850 to >1000 °C, with component creep lives expected to run between 10,000–100,000 hrs, depending on the duty cycle imposed. The need to meet these demands in terms of creep and fatigue life has led to the development of a range of single crystal (SX) nickel based superalloys specifically designed for first and second stage turbine blade applications. First-generation alloys, such as SRR99, have been superseded by second-generation, higher creep strength materials containing additions of Rhenium, such as CMSX-4. These alloys were developed specifically for

aero-engines, where the turbine blades experience for short durations, higher peak temperatures and stresses than are generally found in land based power generation systems. SX castings are susceptible to low and high angle grain boundary defects that can result in low yields and high manufacturing costs. For certain land based turbine duty cycles, it should be possible to use lower cost components, and therefore, a defect tolerant CMSX-4 derivative alloy, called CM186LC has been developed [1-3]. This alloy is intended for use in the as-cast form to minimise solution heat treatment costs and contains grain boundary strengthening additions to overcome defect susceptibility and improve casting yields. Removal of the solution treatment schedule enables a significant cost saving, but results in a complex microstructure containing residual levels of eutectic. The following paper forms part of a large body of research conducted under the COST 522 European collaborative programme, focused on determining the properties of CM186LC SX.

Single crystal superalloy creep modelling:

During service exposure turbine components such as blades and nozzle guide vanes undergo creep and thermo-mechanical fatigue. Utilisation of these components requires that the response of the materials to deformation mechanisms, as a function of engine conditions, be understood. For instance, the creep life has been shown to be highly dependent on operating temperatures; a 10° to 15° increase in temperature can reduce the creep rupture life by 50 % [4]. The single crystal nature of the components used mean that the complex anisotropic response must be included in any model of the elastic or inelastic behaviour. Even though most engine components are cast in the nominally <001> direction, variations in blade orientation occur during casting and the non-uniform shape of components, particularly around cooling holes and platform shoulders, results in a multi-axial stress state and an anisotropic response. For components where the crystal orientation deviates significantly from the <001> direction the need for an anisotropic analysis is even more apparent. This has led to the development by QinetiQ of the UK and NLR of The Netherlands of full 3-D, anisotropic creep deformation materials models which can be used within commercial Finite Element analysis software.

The QinetiQ creep model

Under static loading at elevated temperatures, most engineering materials exhibit a three-stage creep deformation response. It should be possible to describe the creep strain accumulation with an expression involving the stress (σ), temperature (T) and time-on-load (t) as follows:

$$\varepsilon_c = f(\sigma, t, T) \qquad (1)$$

The QinetiQ creep law, based on that first developed by Graham and Walles [5], represents the total creep strain (ε_c) by the sum of a number of independent terms expressed by a power law summation, hence:

$$\varepsilon_c = \sum_j \sum_i \sigma^{\beta_j} t^{\kappa_i} e^{\left(\Lambda_{T\beta_j\kappa_i} T + \Lambda_{S\beta_j\kappa_i}\right)} \qquad (2)$$

where κ_i = 1/3, 1, 3, 9; and β_j is chosen such that the ratio $-\frac{\kappa_i}{\beta_j}$ = ½, ¼, 1/8, 1/16...etc. $\Lambda_{T\beta_j\kappa_i}$ and $\Lambda_{S\beta_j\kappa_i}$ are constants.

The original Graham-Walles equations omitted the rupture term κ_4 = 9, and had a temperature function of the form $(T'_{\beta_j} - T)^{-20\kappa_i}$ where T'_{β_j} are constants. Analysis of a significant creep database has identified a limitation in the form of the temperature term in the original Graham-Walles approach that restricted the predictive accuracy. An exponential function was found to be more accurate over a wide temperature range. A fuller description of the model and the parameter determination methods can be found elsewhere [6].

The NLR creep model

As mentioned previously, under static loading at elevated temperatures, most materials exhibit a three-stage creep deformation response. Moreover, the creep rate is a function of temperature and stress level. These two requirements are met by the creep law presented by Pan, Shollock and McLean [7], which has been applied here.

The shear strain rate at the k-th slip system $\dot{\gamma}^k$ is defined as

$$\dot{\gamma}^k = \dot{\gamma}_i^k (1+\omega^k)(1-S^k) \qquad (3)$$

where ω^k is a dimensionless damage parameter, whose initial value is zero and which evolves with time according to the following relationship:

$$\dot{\omega}^k = \beta^k \dot{\gamma}^k \qquad (4)$$

and S^k is a dimensionless internal stress parameter, whose initial value is also 0 and which evolves with time according to the following:

$$\dot{S}^k = H^k \dot{\gamma}_i^k \left(1 - \frac{S^k}{S_{ss}^k}\right) \qquad (5)$$

The internal stress parameter S controls the primary part of the creep behaviour, whereas the damage parameter ω controls the tertiary part.

The four parameters $\dot{\gamma}_i^k$, β^k, H^k and S_{ss}^k all have the same functional dependence on resolved shear stress and temperature.

$$\dot{\gamma}_i^k = a_1^k \exp\left(b_1^k \tau^k - \frac{Q_1^k}{RT}\right) \qquad (6)$$

$$\beta^k = a_2^k \exp\left(b_2^k \tau^k - \frac{Q_2^k}{RT}\right) \qquad (7)$$

$$H^k = a_3^k \exp\left(b_3^k \tau^k - \frac{Q_3^k}{RT}\right) \qquad (8)$$

$$S_{ss}^k = a_4^k \exp\left(b_4^k \tau^k - \frac{Q_4^k}{RT}\right) \qquad (9)$$

The parameters a_1 to a_4, b_1 to b_4 and Q_1 to Q_4 must be determined for both the octahedral and cuboidal slip systems from experiments.

Single crystal anisotropy

The QinetiQ and NLR Slip System Models assume that all non-linear deformation within a single crystal superalloy occurs on 12 octahedral and 6 cuboidal slip systems (Figure 1). When subjected to a uniaxial load, the degree of slip activity is dependent on the resolved shear stress for that system, determined by the Schmid factor [8] using the following equation:

$$d\tau^{(\alpha)} = \underline{\mu}^{(\alpha)^T} d\underline{\sigma} \qquad (10)$$

where τ is the shear stress, $\underline{\sigma}$ the global stress, and $\underline{\mu}$ are the Schmid factors.

The shear stress τ can be applied within the creep law at the temperature of interest to determine the amount of shear creep deformation γ on the slip system for a given increment of time. The increment of creep strain on a slip system is resolved back into a global strain vector also using the Schmid factors. The contribution from each slip system is resolved and summed to give the total creep strain on the global axes of the model as follows:

$$d\underline{\varepsilon}_C = \sum_{\alpha} \underline{\mu}^{(\alpha)} d\gamma_c^{(\alpha)} \qquad (11)$$

where $d\gamma_c$ is the incremental shear strain on the α slip system and $d\underline{\varepsilon}_c$ is the incremental global creep strain. The general summation covers all 18 slip systems with the contribution from each to the overall global creep strain being determined by the magnitude of the appropriate Schmid factor. By means of substitution the parameters for equation (2) or (6) to (9) are calculated for the octahedral and cube slip systems by using the single shear stress and strain values from equations (10) and (11).

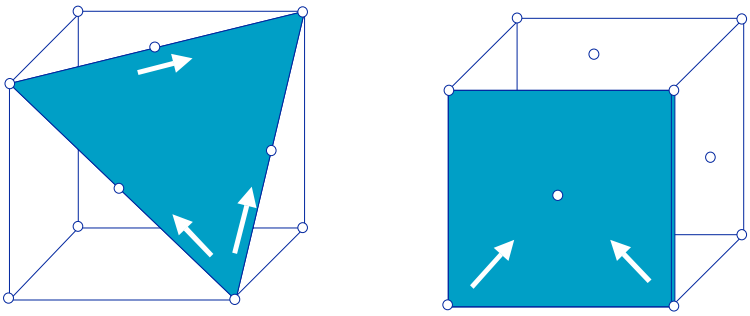

Figure 1. Octahedral and cubic slip systems in a face centred cubic unit cell.

Uniaxial loading along the <001> direction activates 8 identically stressed octahedral systems, the remaining slip systems being subject to zero stress. This allows the associated stress-strain values to be related to single crystal <001> creep test data, and the Λ_S constant in equation (2), or a_i, b_i and Q_i (i =1..4) in equations (6) to (9) for the octahedral slip systems to be determined. Loading along the <111> direction activates 6 identical octahedral systems and 3 identical cubic systems. Having calculated the

octahedral contribution, the Λ_S or a_i, b_i and Q_i for the cubic slip system can be determined.
The octahedral and cuboidal parameters are used to predict the creep deformation on each of the 18 slip systems. Shear strains are transformed onto the global axes to contribute to the incremental creep strain vector, using equation (11).

For an arbitrary orientation the Schmid factors determine the stress component on the individual slip systems from which the creep strain component on each slip system - and hence the creep strain on the global axis - can be calculated.

A computer program has been developed at both QinetiQ and NLR to determine the creep model parameters for the constitutive equations described above. In addition, the constitutive models have been incorporated within user materials subroutines (UMAT's) for ABAQUS and MSC.MARC, for QinetiQ and NLR respectively [9]. Full 3-D isotropic or anisotropic creep strain analysis for a range of stress, temperature and time on load conditions is possible for any pre-defined crystallographic orientation and specimen or aerofoil design.

Results

Analysis of CM186LC creep data

The QinetiQ and NLR creep models have been used to analyse data generated under uniaxial creep at the temperatures 750, 850 and 950 °C for stresses ranging between 115-750 MPa for the crystallographic directions <001> and <111>. These analyses provide the macroscopic creep parameters for the <001> and <111> orientations from which the slip system parameters were calculated. Using the models, the macroscopic creep parameters for the <001> direction can be used to predict the <001> creep behaviour of CM186LC for any stress and temperature. Similarly the macroscopic creep parameters for <111> can be used to predict the <111> creep behaviour for any stress and temperature. A set of predictions have been made for the <001> and <111> directions at 850 °C independently by QinetiQ and NLR, these have been compared with corresponding uniaxial creep test data, generated within the COST 522 Work package 1.1 programme. The predicted and actual uniaxial creep test curves for <001> and <111> at 850 °C and for various stresses are shown in Figures 2 to 5. The data are presented as linear-log plots of creep strain (%) versus time (Hrs), the "M" before the stress in the legend denotes the curves predicted by the model.

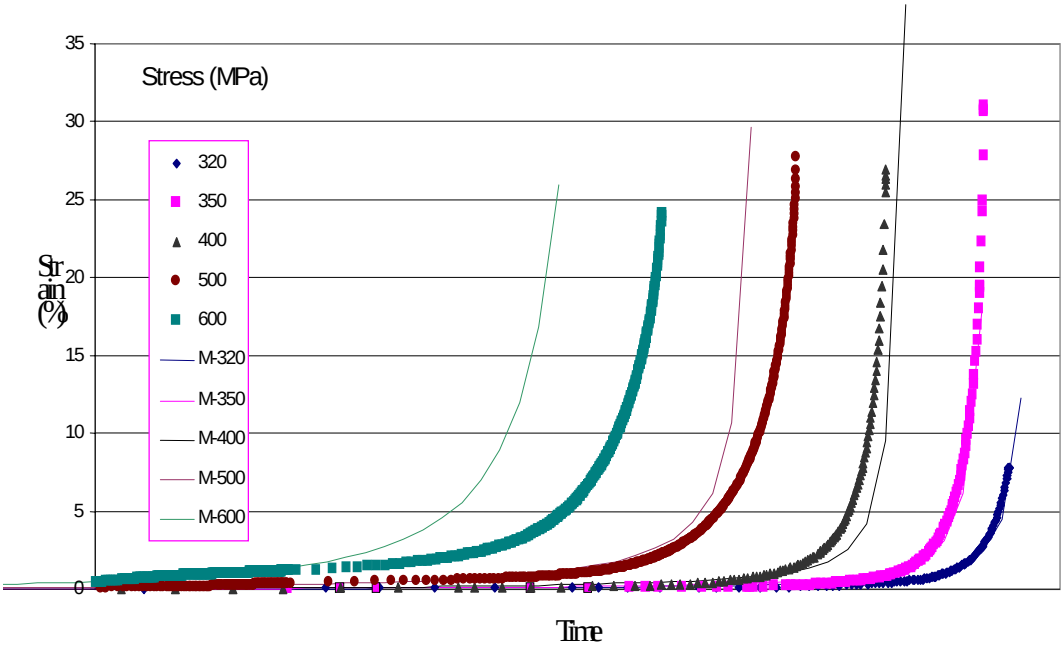

Figure 2. A comparison of uniaxial creep test results and their corresponding curves produced by the QinetiQ creep law model for <001>, 850 °C and various stresses.

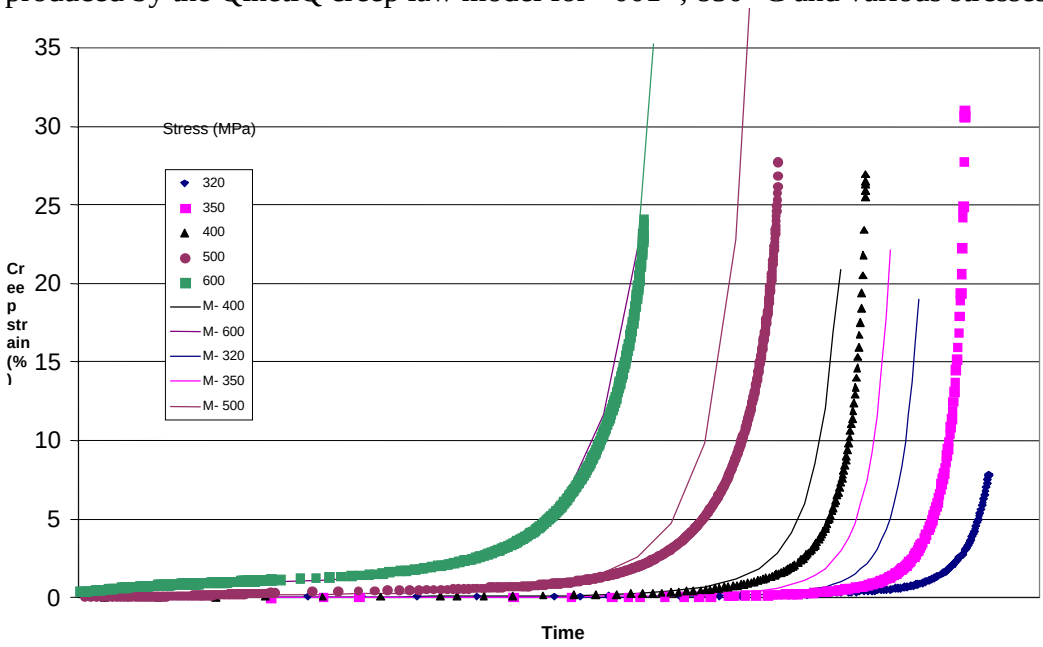

Figure 3. A comparison of uniaxial creep test results and their corresponding curves produced by the NLR creep model for <001>, 850 °C and various stresses.

It can be seen from the comparisons that there is a general agreement between the actual data and the re-plotted, predicted data. The <001> analysis has a closer match than the <111> analysis except for the high stress case (600 MPa) for the QinetiQ model, where

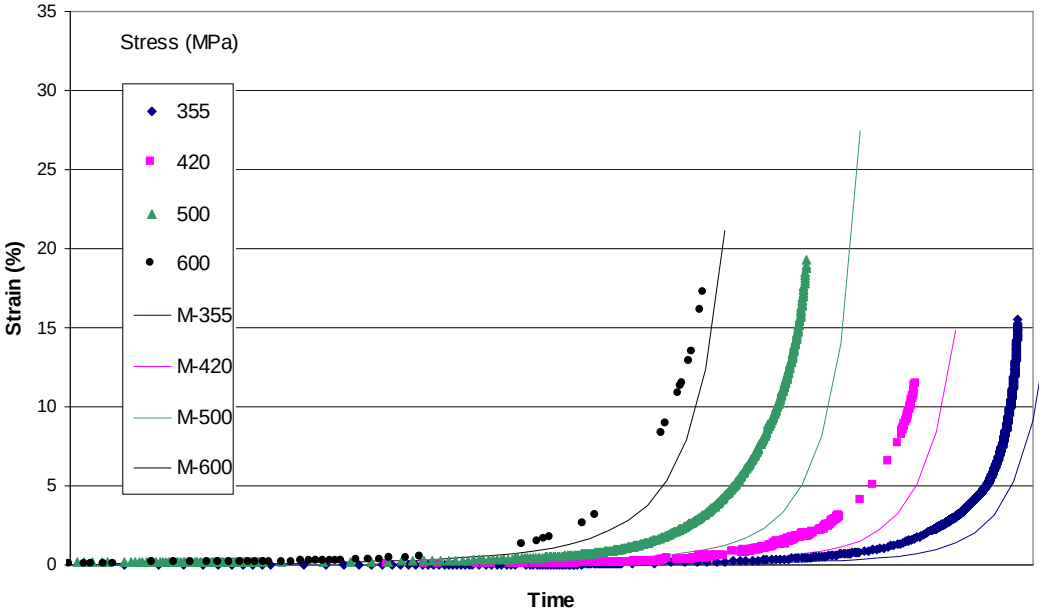

Figure 4. A comparison of uniaxial creep test results and their corresponding curves produced by the QinetiQ creep law model for <111>, 850 °C and various stresses.

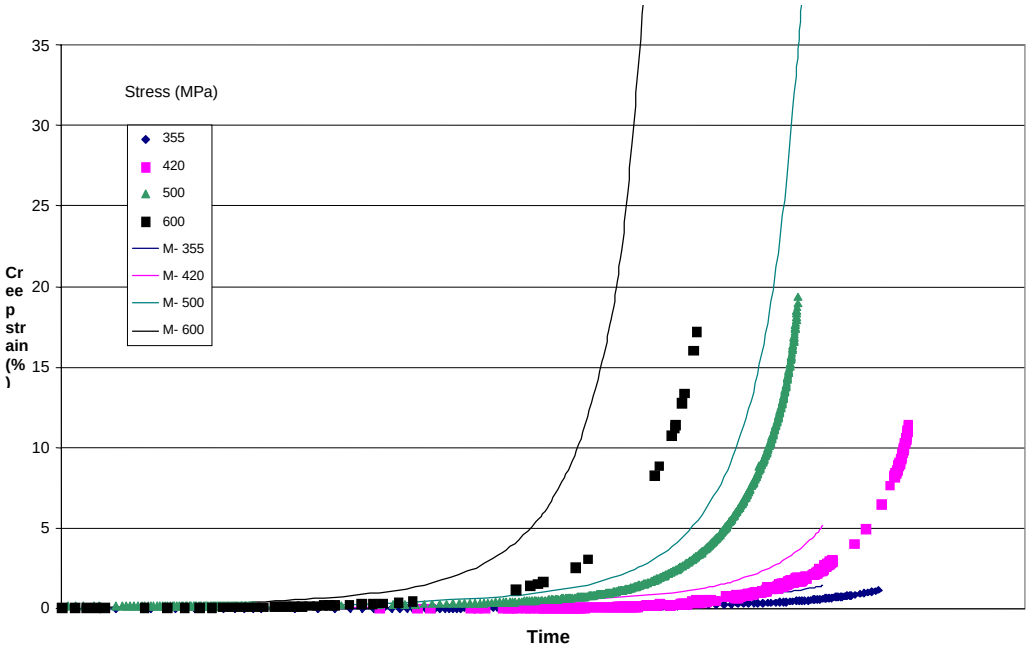

Figure 5. A comparison of uniaxial creep test results and their corresponding curves produced by the NLR creep model for <111>, 850 °C and various stresses.

the prediction begins to breakdown, and conversely in the low stress case (320 MPa) for the NLR model. A comparison between the two models for the <111> direction shows that there is greater agreement.

Finite Element Analysis of creep behaviour

Modelling of diametral strain

When a cylindrical CM186LC SX test bar is loaded in a non-symmetrical direction, the cross section becomes elliptical due to the anisotropic deformation. The NLR creep model was used to calculate this diametral strain distribution, the results of which can be seen in the left-hand side of Figure 6. The Polar plot shown on the right hand side is taken from measurements made from different directions during the course of the creep tests. It can be seen from Figure 6 that the maximum strain is observed in the <001> direction, whereas the minimum is in a <011> direction. This is predicted correctly by the model. Moreover, the absolute value of diametral strain is predicted quite well. Only some details in the shape of the strain distribution are not predicted very well. This may be due to the fact that only a limited number of slip systems is incorporated in the model.

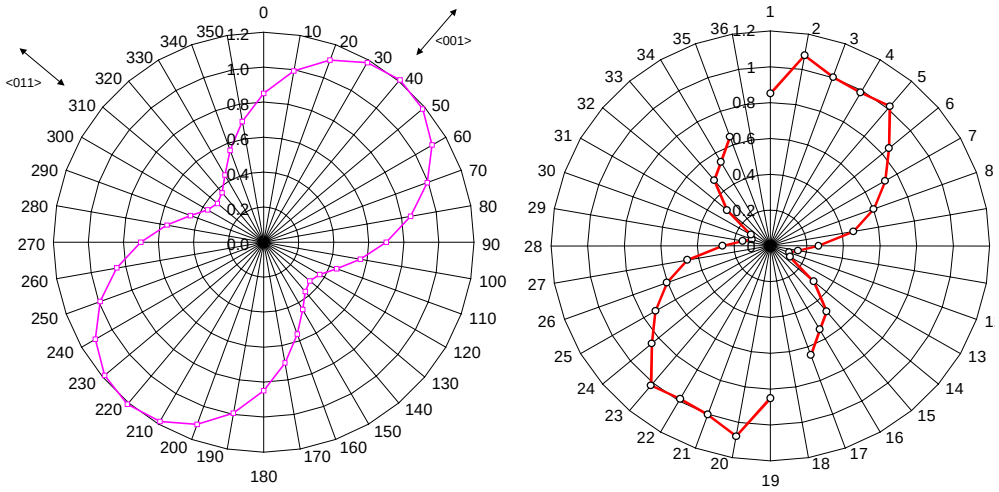

Figure 6. Calculated (left) and measured (right) diametral strain distribution in a cylindrical creep test bar after 875 hrs creep at 850 °C and 355 MPa.

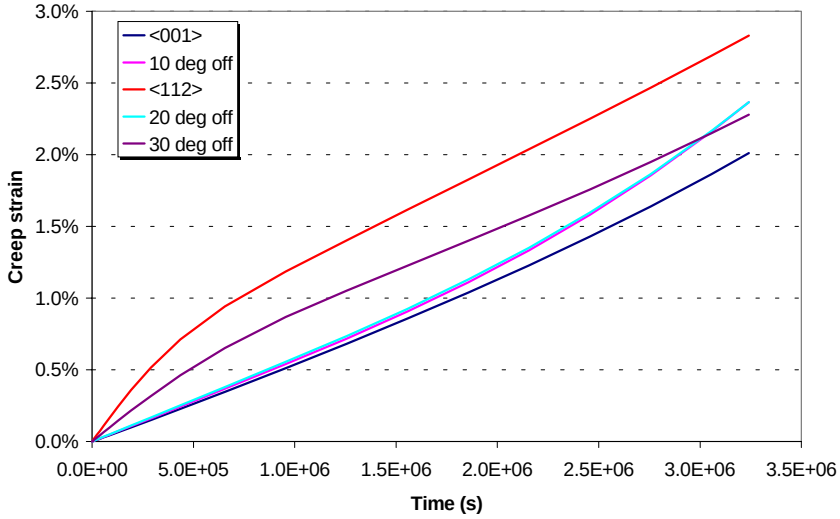

Figure 7 Effect of crystal misorientation on creep behaviour.

Effect of crystal misorientation

For gas turbine applications single crystals are oriented with the superior <001> orientation in the most highly loaded direction (radial direction for turbine rotor blades). However, the alignment of crystal axis and component axis is not always perfect. Figure 7 shows the effect of misorientation of the crystal on creep behaviour. The <001> direction has been shifted towards the <112> direction in steps of 10 degrees along the <001>-<111> boundary line in the stereographic triangle. It appears that the creep rate increases rapidly with increasing misorientation angle, although the increase in creep rate is small between 10 and 20 degrees off the <001> axis.

Creep strain distribution in gas turbine components

The creep strain distribution in a high pressure turbine blade has been calculated, using the NLR model, for a simplified mission (start-up/steady-state at max power/shut-down). The resulting predicted creep damage in terms of Von Mises equivalent creep strain after 100 hrs at max power for an SR99 SX blade and a IN100 polycrystalline blade, for reference, are shown in Figure 8.

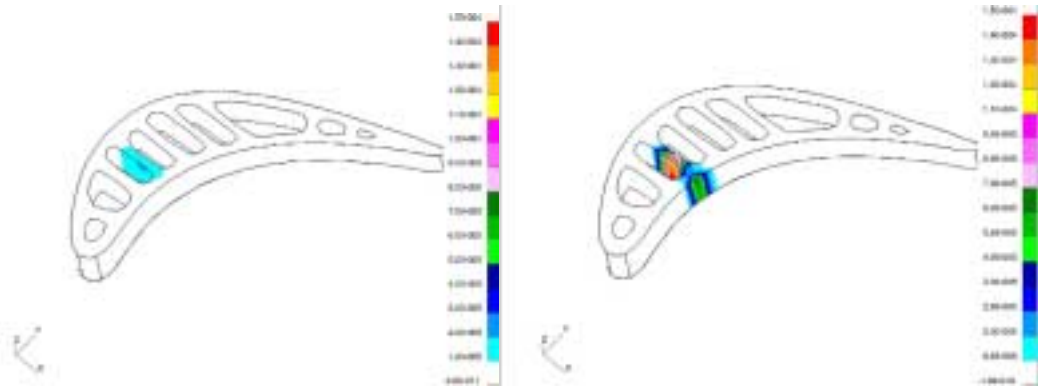

Figure 8. Creep damage in a single crystal (left) and a polycrystalline IN100 blade.

Figure 9 is a picture of the model blade mesh with the creep damage plotted for the isotropic and anisotropic analyses, calculated for a typical industrial gas turbine duty cycle using the QinetiQ creep model. At first sight the results appear fairly similar, though there are important differences (NOTE the blade root is modelled elastically).

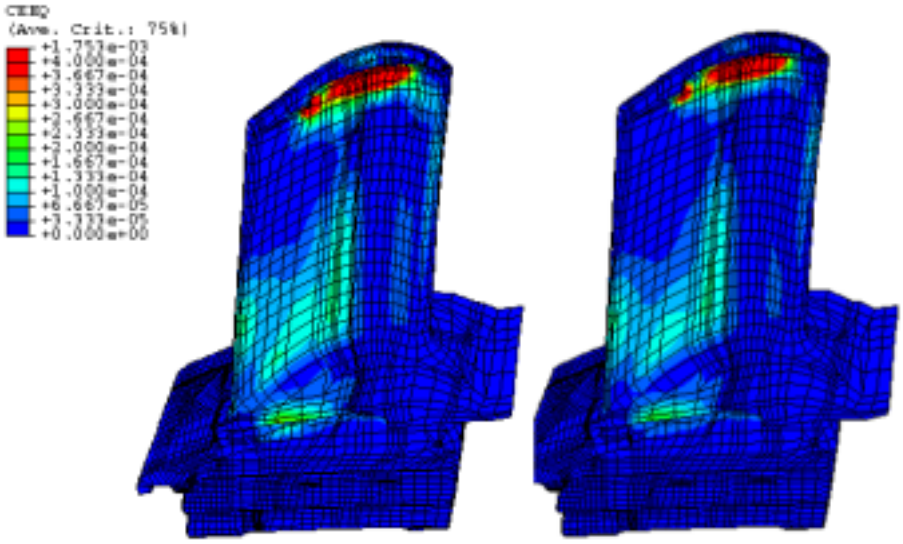

Isotropic Anisotropic

Figure 9. Contour plots of Von Mises Stress - Anisotropic Analysis.

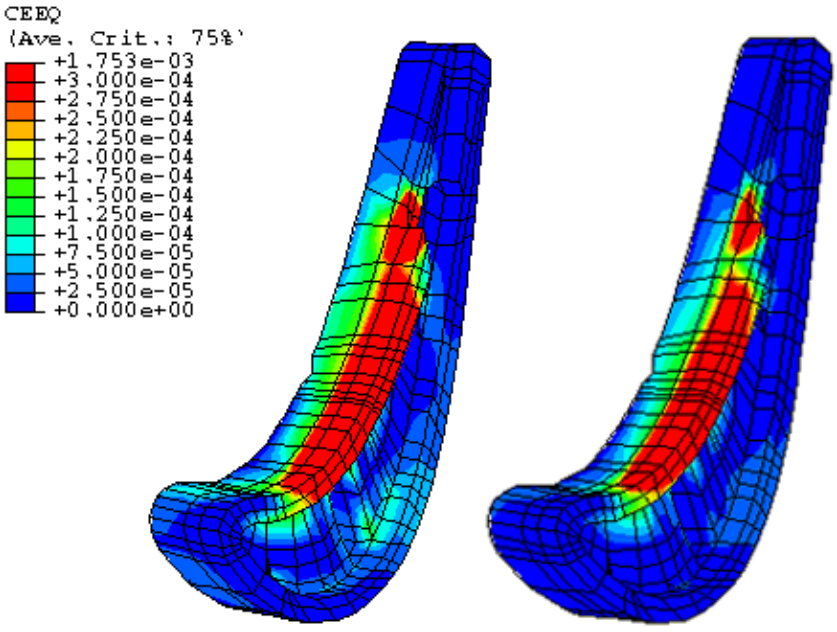

Isotropic Anisotropic

Figure 10. Detail Contour plots of creep damage at tip of aerofoil.

Figures 10 and 11 show the detail at the tip of the aerofoil, where it can be seen that the isotropic analysis predicts a greater degree of creep damage (Fig. 10). As creep strain has the effect of relaxing the stress locally, this explains why the isotropic model predicts a lower Von Mises stress (Fig. 11) distribution.

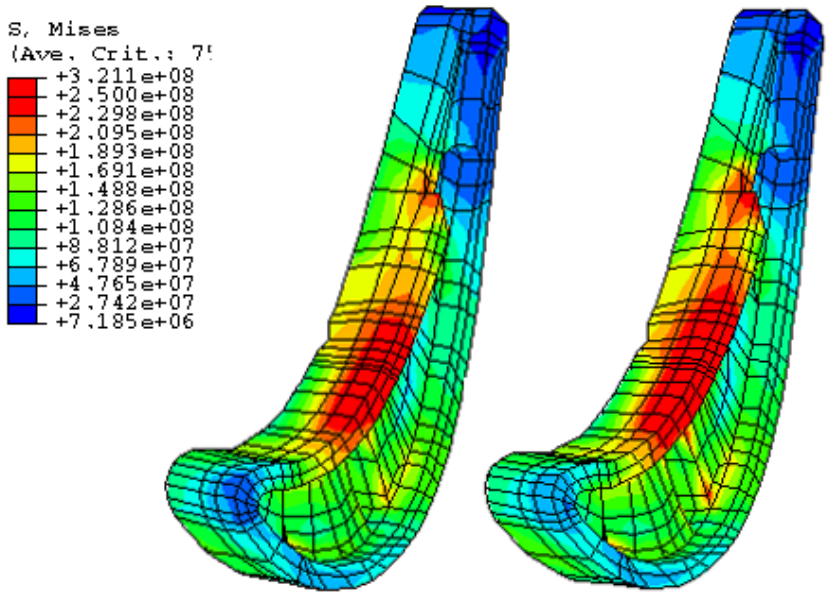

Figure 11. Detail contour plots of Von Mises stress at tip of aerofoil

Discussion:

- Application of the QinetiQ and NLR creep models to modelling the anisotropic creep behaviour of CM186LC SX using a slip system approach has produced similar results. The largest difference between the models is the creep law formulation used by each organisation. However, both formulations are capable of describing the three-stage creep behaviour and therefore predict the CM186LC SX creep deformation quite well.

- Implementation of the anisotropic creep models in finite element codes (ABAQUS and MSC.Marc) offers the potential to conduct a large variety of calculations and simulations that demonstrate the effects of orientation and multiaxial stress states on the deformation response and damage accumulation in complex component geometries. A selection of the simulations available has been presented. Significant differences are found between the predictions due to isotropic and anisotropic formulations specifically located around features such as cooling holes and sharp radii. The results underline the necessity for anisotropic, rather than isotropic analysis, as they show that there are implications for the creep and fatigue life calculations in high pressure turbine blades.

Acknowledgements

QinetiQ and ALSTOM Power gratefully acknowledge the support of UK DTI for this work, NLR acknowledges the support of the Dutch Ministry of Defence. In addition the authors would like to thank CESI, FZ – Jülich, IPM –Brno for the creep data results.

References:

1. K. Harris, J.B. Wahl, “New Superalloy Concepts for Single Crystal Turbine Blade and Vanes”, Proc. 5th Int. Charles Parsons Conf., Cambridge, July 2000, pp. 822-846.
2. P.S. Burkholder, M.C. Thomas, R. Helmink, D.J. Frasier, K. Harris and J.B. Wahl, “CM186 LC Alloy Single Crystal Turbine Vanes” International Gas Turbine and Aeroengine Congress and Exhibition, Indianapolis, June 1999.
3. G. McColvin, J. Sutton, M. Whitehurst, D.G. Fleck, T.A. van Vranken, K. Harris, G.L. Erickson and J.B. Wahl, “Application of the Second Generation DS Superalloy CM186LC to First Stage Turbine Blading in EGT Industrial Turbines”, Proceedings of the 4th International Charles Parsons Conference, November 1997, pp. 339-357.
4. G.F. Harrison, “The Influence of New Materials on Future Engine Design, Component Lifing and Reliability”, Proc. Eurpean Forum, The Royal Aeronautical Society (1993), pp.3.1-3.16.
5. A. Graham and K.J. Walles, Iron and Steel Institute, 179, 1955.
6. T. Homewood, T.J. Ward, M.B. Henderson and G.F. Harrison, “The DERA Slip System Creep Law for the Modelling of Face Centred Cubic Single Crystal Material Behaviour.” Proc. Conf on Modelling of Microstructural Evolution in Creep Resistant Materials, Imperial College, London, September 1998.
7. L-M Pan, B. Shollock, M. McLean, “Modelling of High-Temperature Mechanical Behaviour of a Single Crystal Superalloy”, Proc. R. Soc. Lond. A, 453 (1997), 1689-1715.
8. E. Schmid and W. Boas, Plasticity of Materials, F.A. Hughes & Co, 1950.
9. T.J. Ward and M.B. Henderson, “Writing and Applying a User Material Subroutine (UMAT) for the Analysis of Single Crystal Turbine Blades”, Proc. of the ABAQUS Users Group Conf., September 1998.